



Superplasticity of fine-grained austenitic stainless steels: A review

Hamed Mirzadeh

School of Metallurgy and Materials Engineering, College of Engineering, University of Tehran, Tehran, Iran.

Received: 20 January 2023; Accepted: 4 March 2023

*Corresponding author email: hmirzadeh@ut.ac.ir

ABSTRACT

An appropriate fraction of a second phase for controlling the dynamic grain growth of the fine-grained microstructure during hot deformation can be easily achieved for the high and ultrahigh carbon steels as well as the duplex stainless steels (dual-phase ferritic-austenitic steels), which leads to good superplastic forming behaviors. However, the austenitic stainless steels are typically single-phase alloys at elevated temperatures, which might limit their tensile ductility, and hence, inducing superplastic ductility in these ferrous alloys needs special considerations. In the present review article, firstly, the methods for the grain refinement of austenitic stainless steels are summarized, which includes the formation of deformation-induced martensite during cold deformation and its reversion to austenite at elevated temperatures, severe plastic deformation (SPD) techniques, and thermomechanical processing routes that utilize the dynamic recrystallization (DRX). These methods are used to process fine-grained microstructures that are suitable for activating the grain boundary sliding (GBS) with strain rate sensitivity index (m) of ~ 0.5 at elevated temperatures. Afterward, the reported works on the superplasticity of austenitic stainless steels are critically discussed. It is revealed that the methods such as nitrogen addition, incorporating the carbonitride forming elements such as vanadium, increasing the carbon content of the material for the formation of carbides, and the incomplete reversion treatment for the retention of a small volume fraction of martensite can be used to increase the thermal stability of the ultrafine grained (UFG) microstructure against grain coarsening during superplastic deformation. Finally, some distinct suggestions for future works are introduced.

Keywords: Advanced high-strength steels; Superplasticity; Transformation-induced plasticity effect; Thermomechanical processing; Severe plastic deformation; Grain growth.

1. Introduction

Superplasticity is the ability of a polycrystalline material to exhibit very high elongations prior to failure in a generally isotropic manner, in which the primary deformation mechanism is the grain boundary sliding (GBS) with strain rate sensitivity index (m) of ~ 0.5 [1,2] and the total elongation of at least 200% [3], 300% [4], or 400% [5] is usually expected. As discussed by Langdon [6], the value of 400% can be considered as the most reasonable one for the minimum elongation. This is based on

the experiments on coarse-grained Al-Mg alloys, which showed that the elongations to failure may be up to and slightly exceeding 300% in flow controlled by viscous glide; whereas much higher elongations are attained in a true superplastic condition [6].

In this process, grains slide over each other with the displacement occurring at or very close to their mutual interface. Accordingly, high tensile ductility can be achieved by increasing the number of grains along the tensile axis without the problem

of strain hardening and grain pancaking [6,7]. As shown in Figure 1a, a grain size (d) finer than the projected subgrain size (λ , which inversely depends on the applied stress) is required, for which the stress concentration at the triple junctions can be effectively revealed via the intragranular movement of dislocations in the blocking grain, and then, these intragranular dislocations pile up at the opposing grain boundary and are subsequently removed by a climb into the boundary to enable further GBS [6]. However, for $d > \lambda$, dislocations pile up and climb into the subgrain boundaries, and superplasticity cannot be achieved. Therefore, a fine-grained microstructure is required for achieving superplasticity (typically a grain size less than $10 \mu\text{m}$ is required). In this respect, as shown in Figure 1b, a finer grain size leads to the possibility of achieving superplasticity at higher strain rates ($\dot{\epsilon}$) for faster forming operations [8], where $\dot{\epsilon} \geq 10^{-2} \text{ s}^{-1}$ is considered as high strain rate superplasticity [9]. Finer grain sizes normally lead to higher elongations due to the shorter time available for cavitation [10].

Deformation at elevated temperatures ($T > 0.5T_m$, where T_m is the absolute melting temperature) is required to activate GBS [11]. Therefore, according to the requirement of $d < \lambda$, the thermal stability of the microstructure should be high to inhibit grain

coarsening [12,13]. Consequently, superplastic materials are normally microduplex alloys or pseudo single-phase alloys (having dispersoids as pinning particles) [14]. The microstructure and phase composition of steels are strongly dependent on the content of carbon and other elements as well as the thermomechanical processing conditions. Accordingly, the microstructures might contain austenite (γ), ferrite (α), carbides, and intermetallics [15,16].

A major group of superplastic ferrous materials are the steels with carbon content ranging from 0.4% to the eutectoid point of 0.8% (proeutectoid or high carbon steels) and steels with carbon content above 0.8% (eutectoid or ultrahigh carbon steels) [17]. The superplastic microstructure (normally the spheroidized Fe_3C particles dispersed in a fine-grained α matrix) is usually achieved by the combination of cold/warm/hot working, austenitization/quenching/tempering, and thermal cycling [17-21]. For instance, austenitization of ultrahigh carbon steels in the $\gamma + \text{Fe}_3\text{C}$ region, followed by quenching and tempering at a temperature below A_1 leads to an $\alpha + \text{Fe}_3\text{C}$ microduplex structure with high-angle α boundaries through the recovery of the fine lath martensite + Fe_3C mixture during tempering, which exhibits better superplasticity than that formed by heavy warm rolling or cold rolling and annealing of pearlite that contains higher fraction of low angle boundaries [18]. The superplastic deformation temperature can be above or below the A_1 temperature ($\sim 727 \text{ }^\circ\text{C}$) in the $\gamma + \text{Fe}_3\text{C}$ or $\alpha + \text{Fe}_3\text{C}$ regions, respectively. Tensile deformation in the $\gamma + \text{Fe}_3\text{C}$ region normally leads to lower total elongations, which is related to the more rapid grain growth as a result of the reduced number of cementite particles due to the larger carbon solubility in the γ phase. The optimum carbon content for superplasticity has been reported to be in the range of 1.6 wt% to 1.8 wt% [17]. For steels with lower carbon contents, the amount of Fe_3C particles is lower, leading to relatively more rapid grain growth and loss of superplastic microstructure; while for steels with very high carbon content, the undissolved coarse cementite particles might act as nucleation sites for void formation and a corresponding reduction in the total elongation. It has also been indicated that the addition of cementite-forming elements such as chromium improves superplasticity through the stabilization of the cementite particles [17,22,23].

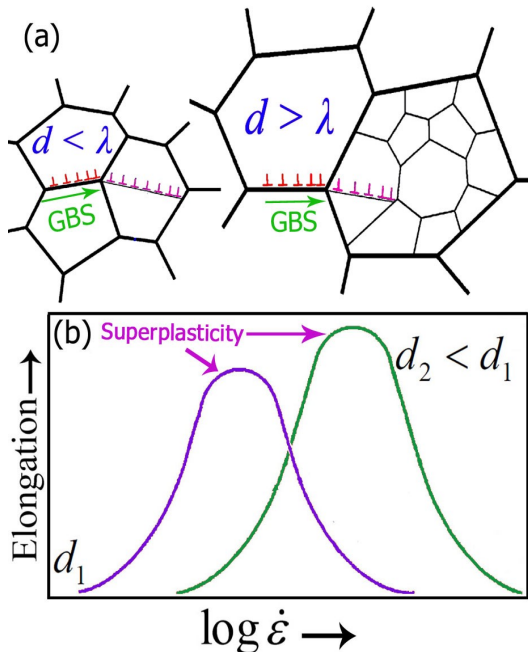


Fig. 1- (a) Unified model for GBS [6] and (b) effect of grain sizes on the plot of total elongation vs. strain rate for a superplastic material [8].

It is noteworthy that the low carbon steels can also be processed to exhibit superplasticity. For instance, grain refinement can be attained by austenitization and quenching, followed by cold rolling and heating at temperatures above the A_3 point. Afterward, superplastic elongations can be achieved at temperatures corresponding to the $\gamma+\alpha$ phase field via formation of a $\gamma+\alpha$ microduplex structure in the intercritical temperature range [17,24]. Similar grain refinement routes of low carbon steels have also been proposed, including the tempering of cold rolled martensite to produce ultrafine grained (UFG) ferrite+carbide aggregate [25-27] and intercritical annealing of cold rolled martensite to process UFG or fine-grained dual phase (DP) steels [28-30].

Duplex stainless steels are the other major group of superplastic steels, showing remarkable superplastic behaviors [31-33]. For obtaining the microduplex structure to induce superplasticity, the sequence of solution treatment at high temperatures (the presence of small amount of the γ phase can suppress the grain coarsening), quenching to obtain a supersaturated ferrite phase at room temperature, and heavy cold rolling is used, which can be followed by annealing at a temperature corresponding to 40-50 vol% γ [17,18,34]. Moreover, as shown in Figure 2, besides the usual peak point for elongation at a

deformation temperature in the conventional two-phase region, another peak point for superplastic elongation might appear at lower temperatures where the intermetallics (such as the σ phase) precipitate dynamically at favorable strain rates in the early stages of deformation [35].

The high and ultrahigh carbon steels as well as the duplex stainless steels have a fraction of a second phase, which can control the dynamic grain growth during superplastic forming. This is an important advantage, which governs their good superplastic behavior during straining at elevated temperatures. However, the austenitic stainless steels are typically single-phase alloys at elevated temperatures, which might limit their tensile ductility. Moreover, contrary to the above mentioned alloys, the austenitic stainless steels do not exhibit any major phase transformation during thermal treatment, and hence, grain refinement needs to be achieved by other techniques. Accordingly, the superplasticity of austenitic stainless steels should be evaluated with the focus on the recent advances on the subject, which is the aim of the present review paper. The superplastic stainless steels might find application in the complicated engineering parts that require fine details. Moreover, the flow stress during superplastic deformation is quite low, which is advantageous. Furthermore, the formed parts have an equiaxed microstructure (due to the operation of GBS as the main deformation mechanism), which is a fine-grained one with good mechanical properties. Therefore, in the following sections, the methods for the grain refinement of austenitic stainless steels are reviewed, and then, the reports on the superplasticity of austenitic stainless steels are summarized.

2. Grain refinement of austenitic stainless steels

Cold deformation and annealing is a viable approach for grain refinement of austenitic stainless steels, which might be considered as the conventional recrystallization annealing of the cold worked structure [36]. However, it is much more complicated. While the austenitic stainless steels do not exhibit any major phase transformation during thermal treatment, cold deformation of metastable grades might lead to the formation of a significant amount of deformation-induced martensite [37-41]. In fact, while the martensite start temperature (M_s) for these steels is usually less than 0 °C, the martensitic transformation is still possible via subjecting the material to sufficient

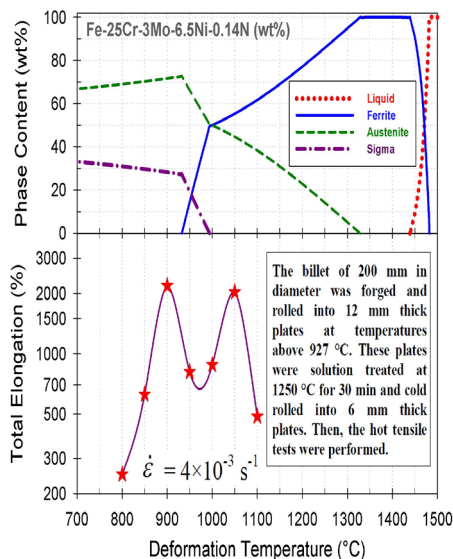


Fig. 2- JMatPro phase predictions and the plot of total elongation vs. deformation temperature for Fe-25Cr-3Mo-6.5Ni-0.14N duplex stainless steel deformed at $4 \times 10^{-3} \text{ s}^{-1}$ (data from [35]).

plastic deformation at low temperatures, where the formation of energetically favorable martensite nucleation sites such as the intersections of shear bands is responsible for this phase transformation [42]. The deformation-induced martensitic transformation depends on many factors such as the chemical composition [43-45], deformation temperature [46-48], grain size [49-52], and strain rate [53-55]. For instance, by consideration of the ASTM grain size number (Gs), the effect of chemical composition (wt%) can be judged based on the concept of $M_{d30/50}$ temperature (the deformation temperature at which 50 vol% deformation-induced martensite forms by true tensile strain of 0.3) [56]:

$$M_{d30/50}(^{\circ}C) = 551 - 462(C + N) - 9.2Si - 8.1Mn - 13.7Cr - 29(Ni + Cu) - 18.5Mo - 68Nb - 1.42(Gs - 8) \quad (1)$$

A lower $M_{d30/50}$ temperature implies higher austenite stability, and hence, increasing the amount of the majority of alloying elements

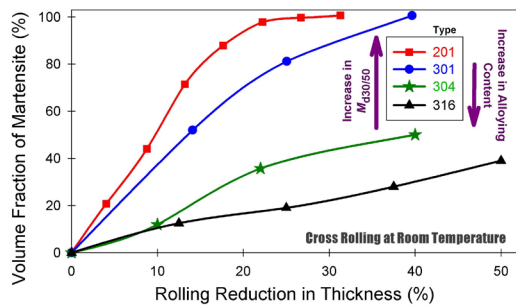


Fig. 3- Martensite formation during rolling [57-60].

enhances the stability of the austenite phase with suppressing the deformation-induced martensitic transformation, as shown in Figure 3 for a number of important grades [57-60]. It can be seen that a high amount of martensite forms in AISI 301 alloy at low reductions in thickness during rolling, but this is not the case for the AISI 316 alloy. In fact, due to the presence of lower amounts of alloying elements, the deformation-induced martensitic transformation is prevalent in the AISI 301 and 304 alloys, but the AISI 316 alloy is much more resistant to this transformation [61,62]. Equation 1 also reveal that the substitution of Ni with Mn increases the $M_{d30/50}$ temperature, and hence, the austenite phase in alloys such as AISI 201 alloy (16-18 wt% Cr – 3.5-5.5 wt% Ni – 5.5-7.5 wt% Mn) [63] is less stable compared to that of AISI 304L alloy, as shown in Figure 3.

During annealing of cold deformed austenitic stainless steels, the processes of reversion of martensite to austenite [64-68] and recrystallization of the retained austenite [69-71] happen. Accordingly, the complete austenitic structure with equiaxed UFG grains can be easily obtained via controlling the annealing process, where the annealing time should be optimized to inhibit grain growth after reversion/recrystallization. Similar methods have also been applied for grain refinement of the low carbon and DP steels [72-75]. Accordingly, the transformation of austenite to deformation-induced martensite during cold deformation is a temporary stage for the grain refinement of metastable austenitic stainless steels, where an example is shown in Figure 4 [76]. According to Tomimura et al. [62], the metastable

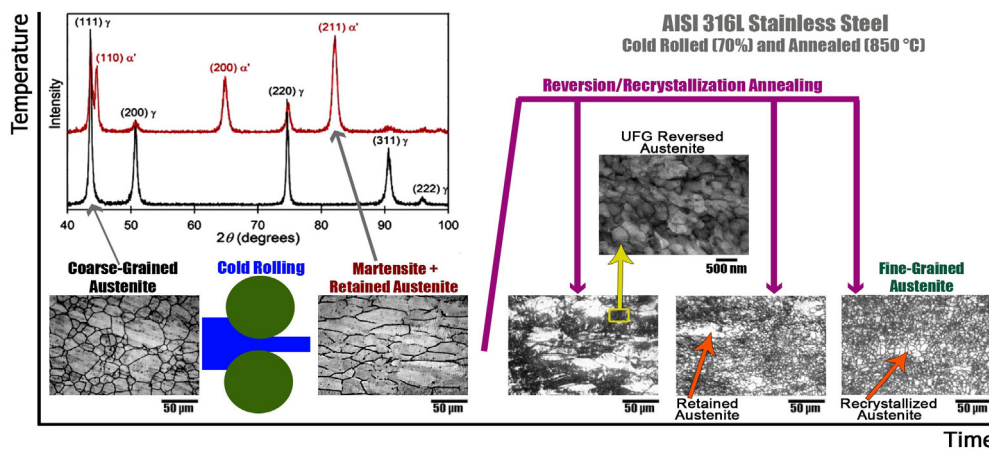


Fig. 4- Formation and reversion of deformation-induced martensite for grain refinement of an austenitic stainless steel [76].

austenite should be almost completely transformed to martensite during the cold rolling stage. In this regard, the Ni equivalent ($\text{Ni} + 0.35\text{Cr}$) of less than 16 wt% might lead to the transformation of more than 90% of austenite to martensite during 90% cold rolling at room temperature. Moreover, most of the martensite phase must revert to austenite at relatively low temperatures where grain growth is difficult to occur (a small amount of martensite phase might be retained). Furthermore, The M_s temperature of the reversed austenite should be below room temperature to stabilize the austenite phase during cooling to room temperature. In this way, a fine-grained and equiaxed austenitic microstructure can be achieved, which might be suitable for superplastic forming, as will be discussed in future sections.

The repetition of the cold rolling and annealing can be used for further grain refinement [77-83]. Moreover, a multi-step annealing approach might be applied for this purpose [84,85]. It should also be mentioned that the situation might become more complicated. For instance, it has been reported that cold rolling of 316L stainless steel has led to the formation of a heterogeneous lamella structure, characterized by coarse grains sandwiched between domains consisting of nano-grains and nano-twins. Upon annealing, a microstructure consisting of nano-grains, nano-twins, lamellar coarse grains, and recrystallized grains was obtained, exhibiting excellent strength-ductility balance [86-89].

Extreme grain refinement can also be achieved by severe plastic deformation (SPD) methods [90-92]. Regarding austenitic stainless steels, the significance of high-pressure torsion (HPT) [93,94], equal-channel angular pressing (ECAP) [95], friction stir processing (FSP) [96], surface mechanical attrition treatment (SMAT) [97,98], multi-directional forging (MDF) [99], and constrained groove pressing (CGP) [100] has been indicated. The mechanism of grain refinement is based on the well-known influence of large plastic deformation on the evolution of microstructure of metallic materials. For instance, the mechanism of

grain refinement of SLM AISI 316L stainless steel via SMAT has been explained, as schematically shown in Figure 5 [98]. SMAT introduces a high density of dislocations, which retards the mobility of dislocations and thereby expedites the initiation of deformation twins and stacking faults. Afterward, dislocation arrays accumulate inside these twins and thereby activate another set of mechanical twins to accommodate plastic deformation. More dislocation loop/tangles arise at twin boundaries across which small misorientations are induced, and subdivision into dislocation cells or low-angle disoriented blocks leads to the formation of low-angle boundaries. Through the formation of dense dislocation walls/dislocation tangles, the misorientation angles gradually increases, transforming into subgrain boundaries. The subgrains further subdivide through a similar mechanism and finally yield grains of nanometer size [98].

Another common method for grain refinement of austenitic stainless steels is the elevated-temperature thermomechanical processing, where dynamic recrystallization (DRX) is a main restoration mechanism [101-103]. Since the stacking fault energy of the austenite phase in austenitic stainless steels is relatively low, the rate of dynamic recovery (DRV) is rather low, and hence, work-hardening can not be balanced only by DRV. Accordingly, the dislocation density gradually increases with strain, and finally the recrystallization starts to occur during deformation upon reaching a critical strain (ϵ_c) [104-106]. The DRX fraction increases with increasing strain, and the full DRX microstructure is eventually obtained (at ϵ_f) [107-109]. As a result, under the condition of single peak flow behavior, a remarkable grain refinement can be achieved by the well-known necklace mechanism [105,106,110]. The dynamically recrystallized grain size (d_{DRX}) is essentially dependent on the deformation temperature and strain rate, which can be represented by the equation of $d_{\text{DRX}} = AZ^{-p}$, where A and p are constants, $Z = \dot{\epsilon} \exp(Q/RT)$ is the Zener-Hollomon parameter, and Q is

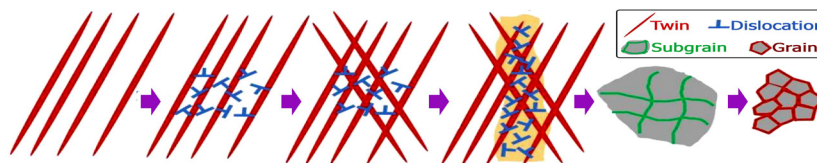


Fig. 5- Schematic representation of the mechanism for nanocrystallization of SLM 316L stainless steel during SMAT [98].

the deformation activation energy [106,110]. Accordingly, in the case of occurrence of DRX, increasing Z leads to a finer d_{DRX} . However, the values of ϵ_c and ϵ_f also increase with increasing Z , and hence, higher strains are required to obtain a fully recrystallized microstructure. These aspects are summarized in the form of DRX map in Figure 6 [110]. For instance, it can be seen that a fine grain size of 5 μm can be obtained at Z value of 10^{17} s^{-1} and ϵ of 3.5 during hot torsion of AISI 304 stainless steel.

3. Superplasticity of austenitic stainless steels

According to the work of Mineura and Tanaka [111], the ultra-high nitrogen stainless steel (UHNSS) with the chemical composition of Fe-20Cr-10Ni-0.7N (wt%) can be subjected to a repeated cold rolling and annealing treatment to induce superplastic behavior at elevated temperatures [111]. Nitrogen is a potent austenite stabilizer and improves the strength at elevated temperatures, but it usually lowers the elongation. However, the precipitation of Cr_2N particles is an important aspect, which might accentuate the superplastic behavior by suppressing the structural coarsening of the fine-grained material. As can be seen in Figure 7a [111], the UHNSS alloy shows higher ductility compared to the low nitrogen alloy, which can be explained based on the presence of Cr_2N particles in the former. The importance of the Cr_2N particles can be better evaluated by consideration of Figure 7b [111], in which the optimum deformation temperatures for large superplastic ductility (i.e. $\sim 800 \text{ }^\circ\text{C}$) are related to

the presence of high amount of Cr_2N phase, and the ductility drops sharply at higher temperatures due to the decline in the amount of the Cr_2N phase. The deformation temperatures lower than $800 \text{ }^\circ\text{C}$ are not appropriate for the activation of the GBS process, leading to low elongations. Accordingly, the superplasticity in the UHNSS alloy largely depends on the presence of fine Cr_2N particles, and hence, the addition of nitrogen by raising the N_2 gas pressure during melting had been a key processing step [17,111].

The amount of Cr_2N phase rapidly decreases at temperatures higher than $800 \text{ }^\circ\text{C}$. Accordingly, for obtaining high superplastic elongation of $\sim 900\%$ at higher temperature of $950 \text{ }^\circ\text{C}$, Astafurova et al. [112] subjected the vanadium-added Fe-19Cr-22Mn-1.5V-0.3C-0.6N (wt%) austenitic stainless steel to a repeated cold rolling and annealing treatment. Afterward, during superplastic deformation, the grain coarsening was suppressed by the more stable V-containing carbonitride precipitates (produced by cold rolling and annealing treatment) as well as precipitate nucleation and growth during high-temperature deformation. The results are summarized in the form of a contour plot of total elongation versus deformation temperature and strain rate in Figure 8, which reveals that high values of tensile ductility can be achieved for low strain rates at $\sim 950 \text{ }^\circ\text{C}$.

As discussed for Figure 7, the fine Cr_2N particles are important microstructural features for obtaining the superplastic ductility in UHNSS alloy. However, the commercial austenitic stainless steels are based on Fe-Cr-Ni system with an austenitic

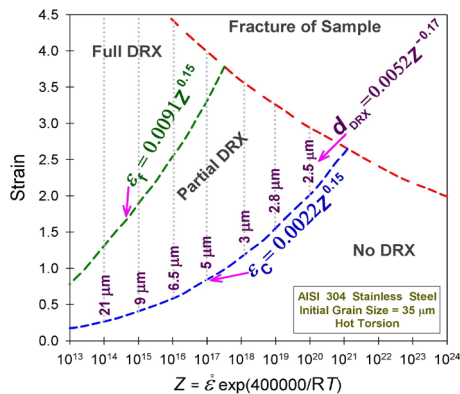


Fig. 6- Hot torsion DRX map of AISI 304 austenitic stainless steel, where the values on dotted lines show the DRX grain size at given Z (redrawn based on [110]).

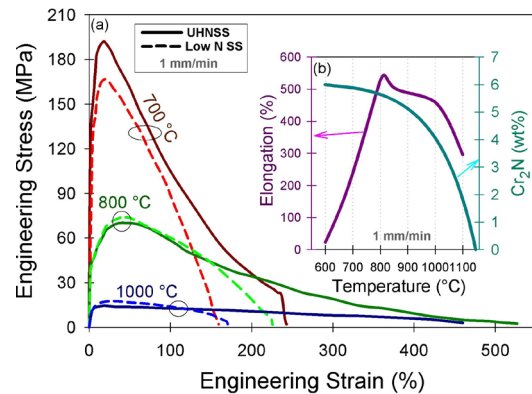


Fig. 7- (a) Tensile stress-strain curves of Fe-20Cr-10Ni-0.7N UHNSS and a low nitrogen grade, (b) the elongation plot of UHNSS alloy and the JMatPro output for the amount of Cr_2N phase (redrawn based on [111]).

microstructure, and hence, the austenite grains abruptly grow during the superplastic deformation, and this prevents further superplastic deformation [113]. For these alloys, the dynamic grain growth of the fine-grained structure during superplastic flow can be controlled by the co-presence of a small amount of the retained deformation-induced martensite at moderate temperatures (such as ~650 °C) [113], for which the kinetics of the reversion of deformation-induced martensite to austenite is slow. The reversion kinetics can be evaluated by consideration of Figure 9 [114], which reveals that a fraction of the deformation-induced martensite remains in the microstructure at temperature of ~650 °C up to reasonable holding times.

The application of this approach for inducing superplasticity in the austenitic stainless steels has been shown by Tsuchiyama et al. [113] for the 18Cr-

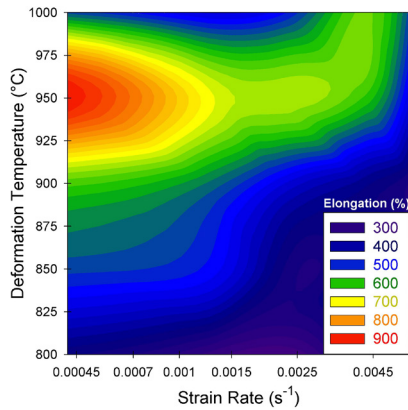


Fig. 8- Contour plot of total elongation versus deformation temperature and strain rate for the Fe-19Cr-22Mn-1.5V-0.3C-0.6N austenitic stainless steel [112].

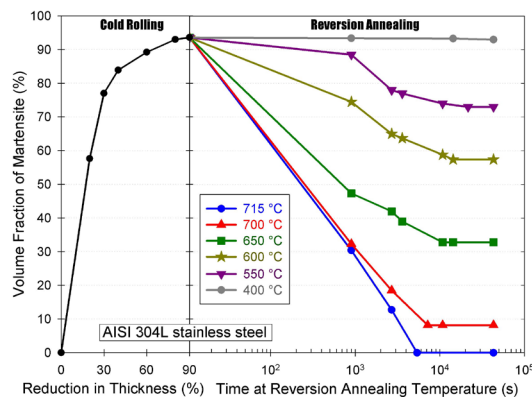


Fig. 9- Formation of martensite during cold rolling and reversion of martensite in the 90% cold rolled sample at different reversion annealing times and temperatures [114].

9Ni stainless steel at 650 °C, Katoh and Torisaka [115,116] for the AISI 304 stainless steel at 700 °C, and Sun et al. [117] for the AISI 304 stainless steel at 650 °C. As shown in Figure 10a, Tsuchiyama et al. [113] showed that the total elongation of 18Cr-9Ni stainless steel at 650 °C is increased with increasing the initial volume fraction of martensite. However, the increase in elongation is leveled off in the range above 15 vol% martensite, which is related to the thermal instability of the martensite phase and its reversion to austenite, as shown in Figure 10b. The dashed lines in this figure reveal that the amount of the martensite phase in the shoulder section is higher than that in the gage section, which reveals that the martensite reversion is promoted by straining. Microstructural analysis revealed that the retention of the fine-grained structure during deformation at 650 °C is highly sensitive to the amount of the retained martensite phase. Accordingly, the co-presence of a small amount of martensite in the UFG structure is essential for improving the thermal stability of the microstructure against grain growth for inducing

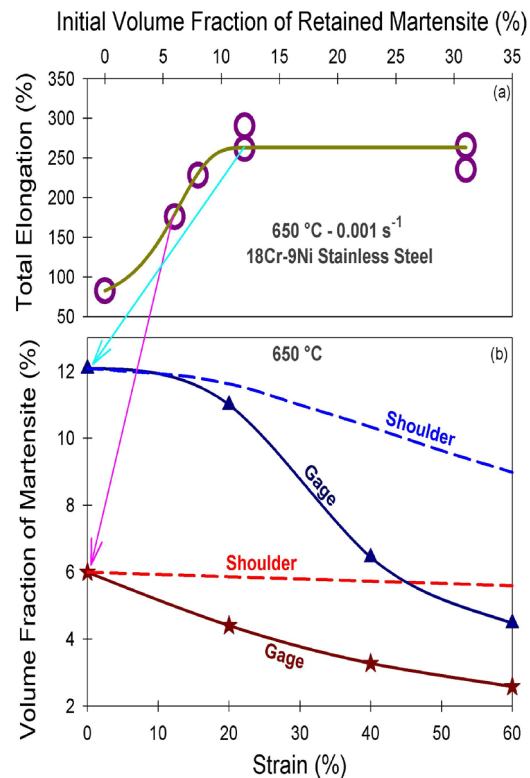


Fig. 10- (a) Total elongation versus the initial volume fraction of retained martensite in 18Cr-9Ni stainless steel and (b) change in the amount of martensite during tensile testing (data from [113]).

the superplastic behavior [113]. Similarly, as shown in Figure 11, Katoh and Torisaka obtained high superplastic elongations in the cold rolled and reversion annealed AISI 304 stainless steel at 700 °C, which was promoted after the repetition of the cold rolling and reversion annealing due to more intense grain refinement [115]. In another study, Sun et al. [117] processed a nano/ultrafine-grained AISI 304 stainless steel with a mean grain size of ~230 nm and ~4 vol% martensite via cold rolling (~93%) followed by reversion annealing treatments at 650 °C for 30 min, which showed superplastic elongations of 296% and more than 300% at deformation temperatures of 630 and 650 °C under strain rate of 0.00025 s⁻¹, respectively. Similar method was also suggested by Xu et al. [118] to induce superplasticity in an 18Cr-8Ni austenitic stainless steel at 800 °C. The elongation of 288% has also been reported by Lu et al. [119] for the tensile deformation of AISI 304 stainless steel at 800 °C.

Superplasticity of austenitic stainless steels

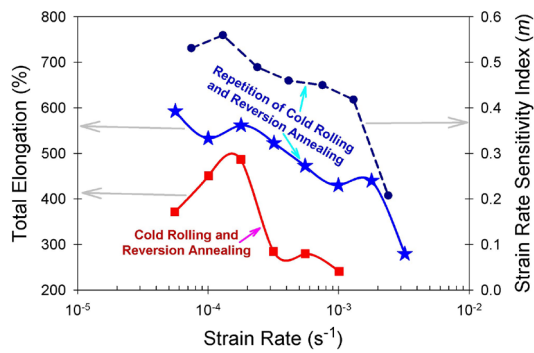


Fig. 11- superplastic elongations and the strain rate sensitivity for the thermomechanically processed AISI 304 stainless steel at 700 °C [115].

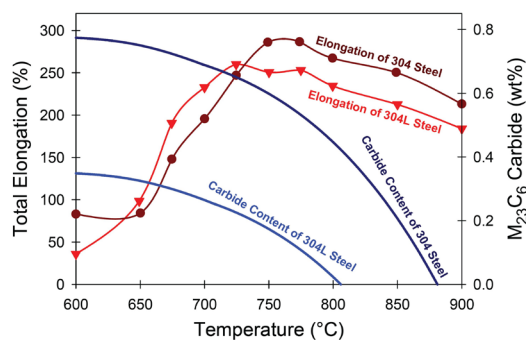


Fig. 12- Tensile elongation versus deformation temperature at strain rate of 0.001 s⁻¹ for the cold rolled AISI 304 and AISI 304L stainless steels that are heated to the test temperature at the heating rate of 35 °C/min as well as the JMatPro predictions for the carbide content [120].

also highly depends on the carbon content of the material. For instance, as shown in Figure 12, Yagodzinsky et al. [120] compared the superplasticity of cold rolled AISI 304 stainless steel (with 0.044 wt% C) with AISI 304L stainless steel (with 0.020 wt% C). It was revealed that the deformation temperature for obtaining maximum elongation in AISI 304 steel with higher carbon content is ~50 °C higher than that for AISI 304L steel, and the total elongation is also higher, which were explained by the presence of carbide particles in the AISI 304 steel that hinders grain growth in austenite.

4. Summary and future prospects

Since the austenitic stainless steels are essentially single-phase materials at the superplastic deformation temperature, the grain growth problem is of utmost importance [121-125]. Accordingly, the N addition for the formation of nitrides [111], the V-N-C addition for the formation of V-containing carbonitrides [112], the incomplete reversion treatment for the retention of a small volume fraction of martensite [113,115,116], and utilizing higher carbon grades for the formation of carbides [120] have been used to increase the thermal stability of the fine-grained microstructure during superplastic deformation. For improving the thermal stability against grain coarsening, much more experimental works are required. In this regard, it has been shown that the presence of molybdenum (Mo) [126] and niobium (Nb) [127] is quite effective in suppressing grain growth of austenitic stainless steels. For instance, as shown in Figure 13 [128], the presence of 2

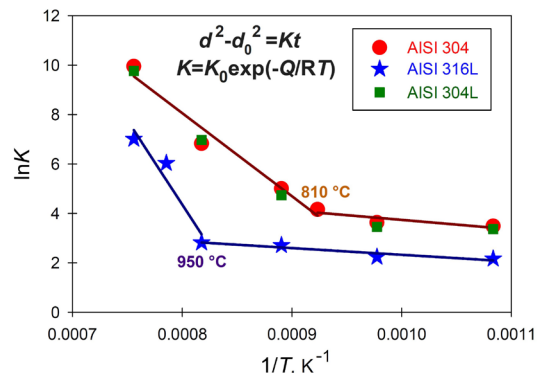


Fig. 13- Activation energy plots to deduce the effect of Mo as an alloying element on the high-temperature behavior of commercial austenitic stainless steels [128].

wt% Mo in the AISI 316 stainless steel has led to the improved thermal stability compared to the AISI 304 stainless steel (~140 °C increase in the grain coarsening temperature). In fact, there is an interaction energy between grain boundaries and solute atoms, which results in the segregation of these atoms to the boundaries and the boundaries have to drag their impurities and can only migrate as fast as the slowly moving impurities [129]. The ascending order of Ni<Cr<V<Ti<Mo<Nb for this retardation effect has been reported for stainless steels [130]. This effect can be advantageous for superplasticity of austenitic stainless steels, which needs to be evaluated.

The reported superplasticity works deal with a limited number of austenitic stainless steels, namely, Fe-20Cr-10Ni-0.7N [111], Fe-19Cr-22Mn-1.5V-0.3C-0.6N [112], 18Cr-9Ni [113], AISI 304 [115-117,119,120], 18Cr-8Ni [118], and AISI 304L [120]. Accordingly, more experimental works are required on AISI 316 grades to study the effect of Mo, and on highly unstable grades (such as AISI 301 [57,78,79] and 201 [58] grades) that are appropriate materials for grain refinement via cold deformation and reversion annealing.

Regarding the application of grain refining methods for inducing superplasticity in the austenitic stainless steels, the reported works are generally based on the thermomechanical processing routes. While the SPD techniques have widely been applied to process superplastic alloys [131-134], more experimental work on the effect of SPD techniques on the superplasticity of austenitic stainless steels is expected in the future. In this regard, it is noteworthy that the methods based on the repetitive corrugation and straightening and CGP can be easily applied on the sheets of austenitic stainless steels for grain refinement [135-137]. Mechanical alloying and consolidation has also been used for processing of superplastic ultrahigh-carbon steel containing 10 wt% Al [138], which showed high strain rate superplasticity. This technique is also effective for the dispersion of particles to inhibit grain coarsening. Moreover, the methods such as HPT can be used for powder consolidation to develop nanocrystalline alloys with a dispersion of nanoparticles [139]. Accordingly, these effective methods can also be assessed for the processing of superplastic austenitic stainless steels. Moreover, the differences between the superplastic materials fabricated by these grain refining methods as well as the advantages/

disadvantages of these fabrication methods should also be investigated. Furthermore, as most of the reported works focused on the inhibition of grain growth during superplastic forming, investigation of the influence of the grain size on the superplastic behavior remains for the future works.

Finally, the superplastic behavior of austenitic stainless steels in the reported works has been assessed by the hot tensile tests. However, the shear punch test (SPT) has also been used for the investigation of the elevated-temperature mechanical properties and the measurement of the strain rate sensitivity index, which is advantageous when only small amounts of materials are available. This technique has been recently used for the assessment of the elevated-temperature mechanical properties and superplasticity of light alloys [131,140-145], and has been applied to austenitic stainless steels for the investigation of mechanical behavior [146-151]. Moreover, the superformability of Mg alloys, low density steels and high-entropy alloys has recently been assessed during compressive loading [152-154], which was found to be a promising technique. Accordingly, these simple and useful techniques can alternatively be applied for investigating the superplasticity of austenitic stainless steels in future works.

References

1. Malik, A., Chaudry, U.M., Hamad, K. and Jun, T.S., 2021. Microstructure Features and Superplasticity of Extruded, Rolled and SPD-Processed Magnesium Alloys: A Short Review. *Metals*, 11(11), p.1766.
2. Mirzadeh, H., 2021. High strain rate superplasticity via friction stir processing (FSP): A review. *Materials Science and Engineering: A*, 819, p.141499.
3. Charit, I. and Mishra, R.S., 2005. Low temperature superplasticity in a friction-stir-processed ultrafine grained Al-Zn-Mg-Sc alloy. *Acta Materialia*, 53(15), pp.4211-4223.
4. Jeong, H.B., Choi, S.W., Kang, S.H. and Lee, Y.K., 2022. Ultralow-temperature superplasticity of high strength Fe-10Mn-3.5 Si steel. *Materials Science and Engineering: A*, p.143408.
5. Wongsan-Ngam, J. and Langdon, T.G., 2022. Advances in superplasticity from a laboratory curiosity to the development of a superplastic forming industry. *Metals*, 12(11), p.1921.
6. Langdon, T.G., 2009. Seventy-five years of superplasticity: historic developments and new opportunities. *Journal of materials science*, 44(22), pp.5998-6010.
7. Kang, S.H., Choi, S.W., Im, Y.D. and Lee, Y.K., 2020. Grain boundary sliding during high-temperature tensile deformation in superplastic Fe-6.6 Mn-2.3 Al steel. *Materials Science and Engineering: A*, 780, p.139174.

8. Xu, C., Furukawa, M., Horita, Z. and Langdon, T.G., 2004. Achieving a superplastic forming capability through severe plastic deformation. *Nanomaterials by Severe Plastic Deformation*, pp.699-710.
9. Higashi, K., Mabuchi, M. and Langdon, T.G., 1996. High-strain-rate superplasticity in metallic materials and the potential for ceramic materials. *ISIJ international*, 36(12), pp.1423-1438.
10. Kawasaki, M. and Langdon, T.G., 2007. Principles of superplasticity in ultrafine-grained materials. *Journal of materials science*, 42(5), pp.1782-1796.
11. Kassner, M.E., 2015. *Fundamentals of creep in metals and alloys*. Butterworth-Heinemann.
12. Motallebi, R., Savaedi, Z. and Mirzadeh, H., 2022. Superplasticity of high-entropy alloys: a review. *Archives of Civil and Mechanical Engineering*, 22(1), pp.1-14.
13. Nguyen, N.T.C., Asghari-Rad, P., Zargaran, A., Kim, E.S., Sathiyamoorthi, P. and Kim, H.S., 2022. Relation of phase fraction to superplastic behavior of multi-principal element alloy with a multi-phase structure. *Scripta Materialia*, 221, p.114949.
14. Giuliano, G. ed., 2011. *Superplastic forming of advanced metallic materials: Methods and applications*. Elsevier.
15. Padmanabhan, K.A., Prabu, S.B., Mulyukov, R.R., Nazarov, A., Imayev, R.M. and Chowdhury, S.G., 2018. Superplasticity: common basis for a near-ubiquitous phenomenon. Springer.
16. Frommeyer, G. and Jiménez, J.A., 2005. Structural superplasticity at higher strain rates of hypereutectoid Fe-5.5 Al-1Sn-1Cr-1.3 C steel. *Metallurgical and Materials Transactions A*, 36(2), pp.295-300.
17. Maehara, Y. and Langdon, T.G., 1990. Superplasticity of steels and ferrous alloys. *Materials Science and Engineering: A*, 128(1), pp.1-13.
18. Furuhashi, T. and Maki, T., 2005. Grain boundary engineering for superplasticity in steels. *Journal of materials science*, 40(4), pp.919-926.
19. Zhang, H., Zhang, L., Cheng, X. and Bai, B., 2010. Superplastic characteristic of Mn-Si-Cr alloyed ultrahigh carbon steel realized through a novel process. *Acta materialia*, 58(18), pp.6173-6180.
20. Özdemir, N. and Orhan, N., 2006. Investigation on the superplasticity behavior of ultrahigh carbon steel. *Materials & design*, 27(8), pp.706-709.
21. Liang, J.W., Shen, Y.F., Misra, R.D.K. and Liaw, P.K., 2021. High strength-superplasticity combination of ultrafine-grained ferritic steel: The significant role of nanoscale carbides. *Journal of Materials Science & Technology*, 83, pp.131-144.
22. Walser, B. and Sherby, O.D., 1979. Mechanical behavior of superplastic ultrahigh carbon steels at elevated temperature. *Metallurgical Transactions A*, 10(10), pp.1461-1471.
23. Wadsworth, J., Lin, J.H. and Sherby, O.D., 1981. Superplasticity in a tool steel. *Metals Technology*, 8(1), pp.190-193.
24. Matsumura, N. and Tokizane, M., 1986. Austenite grain refinement and superplasticity in niobium microalloyed steel. *Transactions of the Iron and Steel Institute of Japan*, 26(4), pp.315-321.
25. Wang, T., Hu, J., Du, L.X., Sun, G.S. and Misra, R.D.K., 2019. Strain rate and temperature dependence of low temperature superplastic deformation in a nanostructured microalloyed steel. *Materials Letters*, 243, pp.165-168.
26. Uejji, R., Tsuji, N., Minamino, Y. and Koizumi, Y., 2002. Ultragrain refinement of plain low carbon steel by cold-rolling and annealing of martensite. *Acta Materialia*, 50(16), pp.4177-4189.
27. Malekjani, S., Timokhina, I.B., Sabirov, I. and Hodgson, P.D., 2009. Deformation behaviour of ultrafine grained steel produced by cold rolling of martensite. *Canadian metallurgical quarterly*, 48(3), pp.229-235.
28. Nakada, N., Arakawa, Y., Park, K.S., Tsuchiyama, T. and Takaki, S., 2012. Dual phase structure formed by partial reversion of cold-deformed martensite. *Materials Science and Engineering: A*, 553, pp.128-133.
29. Azizi-Alizamini, H., Militzer, M. and Poole, W.J., 2011. Formation of ultrafine grained dual phase steels through rapid heating. *ISIJ international*, 51(6), pp.958-964.
30. Alibeyki, M., Mirzadeh, H. and Najafi, M., 2018. Fine-grained dual phase steel via intercritical annealing of cold-rolled martensite. *Vacuum*, 155, pp.147-152.
31. Li, S., Ren, X., Ji, X. and Gui, Y., 2014. Effects of microstructure changes on the superplasticity of 2205 duplex stainless steel. *Materials & Design*, 55, pp.146-151.
32. Miyamoto, H., Mimaki, T. and Hashimoto, S., 2001. Superplastic deformation of micro-specimens of duplex stainless steel. *Materials Science and Engineering: A*, 319, pp.779-783.
33. Sagradi, M., D. Pulino-Sagradi, and R. E. Medrano. "The effect of the microstructure on the superplasticity of a duplex stainless steel." *Acta Materialia* 46, no. 11 (1998): 3857-3862.
34. Han, Y.S. and Hong, S.H., 1999. Microstructural changes during superplastic deformation of Fe-24Cr-7Ni-3Mo-0.14 N duplex stainless steel. *Materials Science and Engineering: A*, 266(1-2), pp.276-284.
35. Maehara, Y. and Ohmori, Y., 1987. Microstructural change during superplastic deformation of δ -ferrite/austenite duplex stainless steel. *Metallurgical and Materials Transactions A*, 18(4), pp.663-672.
36. Humphreys, F.J. and Hatherly, M., 2012. *Recrystallization and related annealing phenomena*. Elsevier.
37. Karjalainen, L.P., Taulavuori, T., Sellman, M. and Kyröläinen, A., 2008. Some strengthening methods for austenitic stainless steels. *Steel research international*, 79(6), pp.404-412.
38. Olson, G.B. and Cohen, M., 1975. Kinetics of strain-induced martensitic nucleation. *Metallurgical transactions A*, 6(4), pp.791-795.
39. De, A.K., Murdock, D.C., Mataya, M.C., Speer, J.G. and Matlock, D.K., 2004. Quantitative measurement of deformation-induced martensite in 304 stainless steel by X-ray diffraction. *Scripta materialia*, 50(12), pp.1445-1449.

40. Mohammadzahi, S. and Mirzadeh, H., 2022. Cold unidirectional/cross-rolling of austenitic stainless steels: a review. *Archives of Civil and Mechanical Engineering*, 22(3), p.129.
41. Ahmedabadi, P.M. and Kain, V., 2020. Kinetics parameters for deformation-induced martensitic transformation in austenitic stainless steels. *Philosophical Magazine Letters*, 100(12), pp.555-560.
42. Lo, K.H., Shek, C.H. and Lai, J.K.L., 2009. Recent developments in stainless steels. *Materials Science and Engineering: R: Reports*, 65(4-6), pp.39-104.
43. Sohrabi, M.J., Naghizadeh, M. and Mirzadeh, H., 2020. Deformation-induced martensite in austenitic stainless steels: a review. *Archives of Civil and Mechanical Engineering*, 20(4), pp.1-24.
44. Pardal, J.M., Tavares, S.S.M., Tavares, M.T., Garcia, P.S.P., Velasco, J.A.C., Abreu, H.F.G. and Pardal, J.P., 2020. Influence of carbon content on the martensitic transformation of titanium stabilized austenitic stainless steels. *The International Journal of Advanced Manufacturing Technology*, 108(1), pp.345-356.
45. Masumura, T., Fujino, K., Tsuchiyama, T., Takaki, S. and Kimura, K., 2021. Effect of Carbon and Nitrogen on Md30 in Metastable Austenitic Stainless Steel. *isij international*, 61(2), pp.546-555.
46. Byun, T.S., Hashimoto, N. and Farrell, K., 2004. Temperature dependence of strain hardening and plastic instability behaviors in austenitic stainless steels. *Acta Materialia*, 52(13), pp.3889-3899.
47. Angel, T., 1954. Formation of martensite in austenitic stainless steels effects of deformation, temperature, and composition. *J. Iron and Steel Inst.*, 177, pp.165-174.
48. Zergani, A., Mirzadeh, H. and Mahmudi, R., 2020. Unraveling the Effect of Deformation Temperature on the Mechanical Behavior and Transformation-Induced Plasticity of the SUS304L Stainless Steel. *Steel Research International*, 91(9), p.2000114.
49. Huang, M., Wang, L., Wang, C., Mogucheva, A. and Xu, W., 2022. Characterization of deformation-induced martensite with various AGSs upon Charpy impact loading and correlation with transformation mechanisms. *Materials Characterization*, 184, p.111704.
50. Sohrabi, M.J., Mirzadeh, H., Sadeghpour, S. and Mahmudi, R., 2023. Grain size dependent mechanical behavior and TRIP effect in a metastable austenitic stainless steel. *International Journal of Plasticity*, 160, p.103502.
51. Kisko, A., Misra, R.D.K., Talonen, J. and Karjalainen, L.P., 2013. The influence of grain size on the strain-induced martensite formation in tensile straining of an austenitic 15Cr-9Mn-Ni-Cu stainless steel. *Materials Science and Engineering: A*, 578, pp.408-416.
52. Sun, G., Zhao, M., Du, L. and Wu, H., 2022. Significant effects of grain size on mechanical response characteristics and deformation mechanisms of metastable austenitic stainless steel. *Materials Characterization*, 184, p.111674.
53. Huang, M., Yuan, J., Wang, J., Wang, L., Mogucheva, A. and Xu, W., 2022. Role of martensitic transformation sequences on deformation-induced martensitic transformation at high strain rates: A quasi in-situ study. *Materials Science and Engineering: A*, 831, p.142319.
54. Talonen, J., Hänninen, H., Nenonen, P. and Pape, G., 2005. Effect of strain rate on the strain-induced $\gamma \rightarrow \alpha'$ -martensite transformation and mechanical properties of austenitic stainless steels. *Metallurgical and materials transactions A*, 36(2), pp.421-432.
55. Das, A., Tarafder, S. and Chakraborti, P.C., 2011. Estimation of deformation induced martensite in austenitic stainless steels. *Materials Science and Engineering: A*, 529, pp.9-20.
56. Nohara, K., Ono, Y. and Ohashi, N., 1977. Composition and grain size dependencies of strain-induced martensitic transformation in metastable austenitic stainless steels. *Tetsu-to-Hagané*, 63(5), pp.772-782.
57. Eskandari, M., Kermanpur, A. and Najafzadeh, A., 2009. Formation of nanocrystalline structure in 301 stainless steel produced by martensite treatment. *Metallurgical and Materials Transactions A*, 40(9), pp.2241-2249.
58. Rezaee, A., Kermanpur, A., Najafzadeh, A., Moallelemi, M. and Baghbadorani, H.S., 2013. Investigation of cold rolling variables on the formation of strain-induced martensite in 201L stainless steel. *Materials & Design*, 46, pp.49-53.
59. Sun, G., Du, L., Hu, J. and Zhang, B., 2020. Significant influence of rolling modes on martensitic transformation, microstructural evolution and texture development in a 304 stainless steel. *Materials Characterization*, 159, p.110073.
60. Mohammadzahi, S., Mirzadeh, H., Sohrabi, M.J., Roostaei, M. and Mahmudi, R., 2023. Elucidating the effects of cold rolling route on the mechanical properties of AISI 316L austenitic stainless steel. *Materials Science and Engineering: A*, 865, p.144616.
61. Naghizadeh, M. and Mirzadeh, H., 2018. Microstructural evolutions during reversion annealing of cold-rolled AISI 316 austenitic stainless steel. *Metallurgical and Materials Transactions A*, 49, pp.2248-2256.
62. Tomimura, K., Takaki, S., Tanimoto, S. and Tokunaga, Y., 1991. Optimal chemical composition in Fe-Cr-Ni alloys for ultra grain refining by reversion from deformation induced martensite. *ISIJ international*, 31(7), pp.721-727.
63. Souza Filho, I.R.D., Zilnyk, K.D., Sandim, M.J.R., Bolmaro, R.E. and Sandim, H.R.Z., 2017. Strain partitioning and texture evolution during cold rolling of AISI 201 austenitic stainless steel. *Materials Science and Engineering: A*, 702, pp.161-172.
64. Misra, R.D.K., Challa, V.S.A. and Injeti, V.S.Y., 2022. Phase reversion-induced nanostructured austenitic alloys: an overview. *Materials Technology*, 37(7), pp.437-449.
65. Järvenpää, A., Jaskari, M., Kisko, A. and Karjalainen, P., 2020. Processing and properties of reversion-treated austenitic stainless steels. *Metals*, 10(2), p.281.
66. Panov, D., Kudryavtsev, E., Chernichenko, R., Smirnov, A., Stepanov, N., Simonov, Y., Zherebtsov, S. and Salishchev, G., 2021. Mechanisms of the reverse martensite-to-austenite

- transformation in a metastable austenitic stainless steel. *Metals*, 11(4), p.599.
67. Padilha, A.F., Plaut, R.L. and Rios, P.R., 2003. Annealing of cold-worked austenitic stainless steels. *ISIJ international*, 43(2), pp.135-143.
68. Tomimura, K., Takaki, S. and Tokunaga, Y., 1991. Reversion mechanism from deformation induced martensite to austenite in metastable austenitic stainless steels. *ISIJ international*, 31(12), pp.1431-1437.
69. Sun, G.S., Du, L.X., Hu, J. and Misra, R.D.K., 2018. Microstructural evolution and recrystallization behavior of cold rolled austenitic stainless steel with dual phase microstructure during isothermal annealing. *Materials Science and Engineering: A*, 709, pp.254-264.
70. Kisko, A., Hamada, A.S., Talonen, J., Porter, D. and Karjalainen, L.P., 2016. Effects of reversion and recrystallization on microstructure and mechanical properties of Nb-alloyed low-Ni high-Mn austenitic stainless steels. *Materials Science and Engineering: A*, 657, pp.359-370.
71. Xu, D.M., Li, G.Q., Wan, X.L., Misra, R.D.K., Zhang, X.G., Xu, G. and Wu, K.M., 2018. The effect of annealing on the microstructural evolution and mechanical properties in phase reversed 316LN austenitic stainless steel. *Materials Science and Engineering: A*, 720, pp.36-48.
72. Tasan, C.C., Diehl, M., Yan, D., Bechtold, M., Roters, F., Schemmann, L., Zheng, C., Peranio, N., Ponge, D., Koyama, M. and Tsuzaki, K., 2015. An overview of dual-phase steels: advances in microstructure-oriented processing and micromechanically guided design. *Annual Review of Materials Research*, 45, pp.391-431.
73. Nasiri, Z., Ghaemifar, S., Naghizadeh, M. and Mirzadeh, H., 2021. Thermal mechanisms of grain refinement in steels: a review. *Metals and Materials International*, 27(7), pp.2078-2094.
74. Mazaheri, Y., Jahanara, A.H., Sheikhi, M. and Kalashami, A.G., 2019. High strength-elongation balance in ultrafine grained ferrite-martensite dual phase steels developed by thermomechanical processing. *Materials Science and Engineering: A*, 761, p.138021.
75. Najafi, M., Mirzadeh, H. and Alibeyki, M., 2019. Improved mechanical properties of structural steel via developing bimodal grain size distribution and intercritical heat treatment. *Journal of Materials Engineering and Performance*, 28(9), pp.5409-5414.
76. Kheiri, S., Mirzadeh, H. and Naghizadeh, M., 2019. Tailoring the microstructure and mechanical properties of AISI 316L austenitic stainless steel via cold rolling and reversion annealing. *Materials Science and Engineering: A*, 759, pp.90-96.
77. Ma, Y., Jin, J.E. and Lee, Y.K., 2005. A repetitive thermomechanical process to produce nano-crystalline in a metastable austenitic steel. *Scripta Materialia*, 52(12), pp.1311-1315.
78. Al-Fadhalah, K.J., Al-Attal, Y. and Rafeeq, M.A., 2022. Microstructure Refinement of 301 Stainless Steel via Thermomechanical Processing. *Metals*, 12(10), p.1690.
79. Hamada, A., Khosravifard, A., Ghosh, S., Jaskari, M., Järvenpää, A. and Karjalainen, P., 2022. High-speed erichsen testing of grain-refined 301LN austenitic stainless steel processed by double-reversion annealing. *Metallurgical and Materials Transactions A*, 53(6), pp.2174-2194.
80. Naghizadeh, M. and Mirzadeh, H., 2018. Processing of fine grained AISI 304L austenitic stainless steel by cold rolling and high-temperature short-term annealing. *Materials Research Express*, 5(5), p.056529.
81. Mandal, S., Bhaduri, A.K. and Subramanya Sarma, V., 2011. One-step and iterative thermo-mechanical treatments to enhance $\Sigma 3n$ boundaries in a Ti-modified austenitic stainless steel. *Journal of Materials Science*, 46(1), pp.275-284.
82. Sun, G.S., Du, L.X., Hu, J., Xie, H., Wu, H.Y. and Misra, R.D.K., 2015. Ultrahigh strength nano/ultrafine-grained 304 stainless steel through three-stage cold rolling and annealing treatment. *Materials characterization*, 110, pp.228-235.
83. He, Y.M., Wang, Y.H., Guo, K. and Wang, T.S., 2017. Effect of carbide precipitation on strain-hardening behavior and deformation mechanism of metastable austenitic stainless steel after repetitive cold rolling and reversion annealing. *Materials Science and Engineering: A*, 708, pp.248-253.
84. Nanda, T., Kumar, B.R. and Singh, V., 2016. A Thermal Cycling Route for Processing Nano-grains in AISI 316L Stainless Steel for Improved Tensile Deformation Behaviour. *Defence Science Journal*, 66(5).
85. Ravi Kumar, B. and Sharma, S., 2014. Recrystallization behavior of a heavily deformed austenitic stainless steel during iterative type annealing. *Metallurgical and Materials Transactions A*, 45(13), pp.6027-6038.
86. Li, J., Cao, Y., Gao, B., Li, Y. and Zhu, Y., 2018. Superior strength and ductility of 316L stainless steel with heterogeneous lamella structure. *Journal of Materials Science*, 53(14), pp.10442-10456.
87. Li, J., Gao, B., Huang, Z., Zhou, H., Mao, Q. and Li, Y., 2018. Design for strength-ductility synergy of 316L stainless steel with heterogeneous lamella structure through medium cold rolling and annealing. *Vacuum*, 157, pp.128-135.
88. Wang, S., Li, J., Cao, Y., Gao, B., Mao, Q. and Li, Y., 2018. Thermal stability and tensile property of 316L stainless steel with heterogeneous lamella structure. *Vacuum*, 152, pp.261-264.
89. Li, J., Mao, Q., Chen, M., Qin, W., Lu, X., Liu, T., She, D., Kang, J., Wang, G., Zhu, X. and Li, Y., 2021. Enhanced pitting resistance through designing a high-strength 316L stainless steel with heterostructure. *Journal of Materials Research and Technology*, 10, pp.132-137.
90. Edalati, K., Bachmaier, A., Beloshenko, V.A., Beygelzimer, Y., Blank, V.D., Botta, W.J., Bryła, K., Čížek, J., Divinski, S., Enikeev, N.A., Estrin, Y., Faraji, G., Figueiredo, R.B., Fuji, M., Furuta, T., Grosdidier, T., Gubicza, J., Hohenwarther, A., Horita, Z., Huot, J., Ikoma, Y., Janeček, M., Kawasaki, M., Král, P., Kuramoto, S., Langdon, T.G., Leiva, D.R., Levitas, V.I., Mazilkina, A., Mito, M., Miyamoto, H., Nishizaki, T., Pippin, R., Popov, V.V., Popova, E.N., Purcek, G., Renk, O., Révész, A., Sauvage, X., Sklenicka, V., Skrotzki, W., Straumal, B.B., Suwas, S., Toth, L.S., Tsuji, N., Valiev, R.Z., Wilde, G., Zehetbauer, M.J., and Zhu, X., 2022. Nanomaterials by severe plastic deformation: review of historical developments and recent advances. *Materials Research Let-*

- ters, 10(4), pp.163-256.
91. Cao, Y., Ni, S., Liao, X., Song, M. and Zhu, Y., 2018. Structural evolutions of metallic materials processed by severe plastic deformation. *Materials Science and Engineering: R: Reports*, 133, pp.1-59.
92. Heidarzadeh, A., Mironov, S., Kaibyshev, R., Çam, G., Simar, A., Gerlich, A., Khodabakhshi, F., Mostafaei, A., Field, D.P., Robson, J.D., Deschamps, A., and Withers, P.J., 2021. Friction stir welding/processing of metals and alloys: a comprehensive review on microstructural evolution. *Progress in Materials Science*, 117, p.100752.
93. Scheriau, S., Zhang, Z., Kleber, S. and Pippan, R., 2011. Deformation mechanisms of a modified 316L austenitic steel subjected to high pressure torsion. *Materials Science and Engineering: A*, 528(6), pp.2776-2786.
94. Gubicza, J., El-Tahawy, M., Huang, Y., Choi, H., Choe, H., Lábár, J.L. and Langdon, T.G., 2016. Microstructure, phase composition and hardness evolution in 316L stainless steel processed by high-pressure torsion. *Materials Science and Engineering: A*, 657, pp.215-223.
95. Qu, S., Huang, C.X., Gao, Y.L., Yang, G., Wu, S.D., Zang, Q.S. and Zhang, Z.F., 2008. Tensile and compressive properties of AISI 304L stainless steel subjected to equal channel angular pressing. *Materials Science and Engineering: A*, 475(1-2), pp.207-216.
96. Sajadifar, S.V., Hosseinzadeh, A., Richter, J., Krochmal, M., Wegener, T., Bolender, A., Heidarzadeh, A., Niendorf, T. and Yapici, G.G., 2022. On the Friction Stir Processing of Additive-Manufactured 316L Stainless Steel. *Advanced Engineering Materials*, 24(10), p.2200384.
97. Zhang, H.W., Hei, Z.K., Liu, G., Lu, J. and Lu, K., 2003. Formation of nanostructured surface layer on AISI 304 stainless steel by means of surface mechanical attrition treatment. *Acta materialia*, 51(7), pp.1871-1881.
98. Ghosh, S., Bibhanshu, N., Suwas, S. and Chatterjee, K., 2021. Surface mechanical attrition treatment of additively manufactured 316L stainless steel yields gradient nanostructure with superior strength and ductility. *Materials Science and Engineering: A*, 820, p.141540.
99. Nakao, Y. and Miura, H., 2011. Nano-grain evolution in austenitic stainless steel during multi-directional forging. *Materials Science and Engineering: A*, 528(3), pp.1310-1317.
100. Singh, R., Agrahari, S., Yadav, S.D. and Kumar, A., 2021. Microstructural evolution and mechanical properties of 316 austenitic stainless steel by CGP. *Materials Science and Engineering: A*, 812, p.141105.
101. Salvatori, I., Inoue, T. and Nagai, K., 2002. Ultrafine grain structure through dynamic recrystallization for Type 304 stainless steel. *ISIJ international*, 42(7), pp.744-750.
102. Kim, S.I. and Yoo, Y.C., 2001. Dynamic recrystallization behavior of AISI 304 stainless steel. *Materials Science and Engineering: A*, 311(1-2), pp.108-113.
103. Souza, R.C., Silva, E.S., Jorge Jr, A.M., Cabrera, J.M. and Balancin, O., 2013. Dynamic recovery and dynamic recrystallization competition on a Nb-and N-bearing austenitic stainless steel biomaterial: Influence of strain rate and temperature. *Materials Science and Engineering: A*, 582, pp.96-107.
104. Tamura, I., Sekine, H. and Tanaka, T., 2013. Thermomechanical processing of high-strength low-alloy steels. Butterworth-Heinemann.
105. Zhang, H.K., Xiao, H., Fang, X.W., Zhang, Q., Logé, R.E. and Huang, K., 2020. A critical assessment of experimental investigation of dynamic recrystallization of metallic materials. *Materials & Design*, 193, p.108873.
106. Savaedi, Z., Motallebi, R. and Mirzadeh, H., 2022. A review of hot deformation behavior and constitutive models to predict flow stress of high-entropy alloys. *Journal of Alloys and Compounds*, 903, p.163964.
107. Mandal, S., Bhaduri, A.K. and Subramanya Sarma, V., 2012. Influence of state of stress on dynamic recrystallization in a titanium-modified austenitic stainless steel. *Metallurgical and Materials Transactions A*, 43(2), pp.410-414.
108. Belyakov, A., Tikhonova, M., Dolzhenko, P., Sakai, T. and Kaibyshev, R., 2019. On kinetics of grain refinement and strengthening by dynamic recrystallization. *Advanced Engineering Materials*, 21(1), p.1800104.
109. Motallebi, R., Savaedi, Z. and Mirzadeh, H., 2022. Additive manufacturing—A review of hot deformation behavior and constitutive modeling of flow stress. *Current Opinion in Solid State and Materials Science*, 26(3), p.100992.
110. Dehghan-Manshadi, A., Barnett, M.R. and Hodgson, P.D., 2008. Hot deformation and recrystallization of austenitic stainless steel: Part I. Dynamic recrystallization. *Metallurgical and Materials Transactions A*, 39(6), pp.1359-1370.
111. Mineura, K. and Tanaka, K., 1989. Superplasticity of 20Cr–10Ni–0.7 N (wt%) ultra-high nitrogen austenitic stainless steel. *Journal of materials science*, 24(8), pp.2967-2970.
112. Astafurova, E., Moskvina, V., Panchenko, M., Maier, G., Melnikov, E., Reunova, K., Galchenko, N. and Astafurov, S., 2019. On the Superplastic Deformation in Vanadium-Alloyed High-Nitrogen Steel. *Metals*, 10(1), p.27.
113. Tsuchiyama, T., Nakamura, Y., Hidaka, H. and Takaki, S., 2004. Effect of initial microstructure on superplasticity in ultrafine grained 18Cr-9Ni stainless steel. *Materials transactions*, 45(7), pp.2259-2263.
114. Sohrabi, M.J., Mirzadeh, H. and Dehghanian, C., 2020. Thermodynamics basis of saturation of martensite content during reversion annealing of cold rolled metastable austenitic steel. *Vacuum*, 174, p.109220.
115. Katoh, M. and Torisaka, Y., 1998. Thermo-mechanical treatment for improvement of superplasticity of SUS304. *Tetsu-to-Hagané*, 84(2), pp.127-130.
116. Katoh, M. and Torisaka, Y., 2003. Thermo-mechanical Treatment with Multi-direction Upsetting for Improvement of Superplasticity in SUS304. *Tetsu-to-Hagané*, 89(10), pp.1038-1043.
117. Sun, G.S., Du, L.X., Hu, J., Xie, H. and Misra, R.D.K., 2017.

- Low temperature superplastic-like deformation and fracture behavior of nano/ultrafine-grained metastable austenitic stainless steel. *Materials & Design*, 117, pp.223-231.
118. Xu, D.M., Li, G.Q., Wan, X.L., Misra, R.D.K., Yu, J.X. and Xu, G., 2020. On the deformation mechanism of austenitic stainless steel at elevated temperatures: A critical analysis of fine-grained versus coarse-grained structure. *Materials Science and Engineering: A*, 773, p.138722.
119. Lu, J., Zhao, M., Wu, H. and Du, L., 2022. Effect of Warm Deformation on Mechanical Properties and Deformation Mechanism of Nano/Ultrafine-Grained 304 Stainless Steel. *steel research international*, 93(10), p.2200198.
120. Yagodzinskyy, Y., Pimenoff, J., Tarasenko, O., Romu, J., Nenonen, P. and Hänninen, H., 2004. Grain refinement processes for superplastic forming of AISI 304 and 304L austenitic stainless steels. *Materials science and technology*, 20(7), pp.925-929.
121. Shirdel, M., Mirzadeh, H. and Habibi Parsa, M., 2014. Microstructural evolution during normal/abnormal grain growth in austenitic stainless steel. *Metallurgical and Materials Transactions A*, 45(11), pp.5185-5193.
122. Stornelli, G., Gaggiotti, M., Mancini, S., Napoli, G., Rocchi, C., Tirasso, C. and Di Schino, A., 2022. Recrystallization and grain growth of AISI 904L super-austenitic stainless steel: A multivariate regression approach. *Metals*, 12(2), p.200.
123. Kotan, H. and Darling, K.A., 2018. A study of microstructural evolution of Fe-18Cr-8Ni, Fe-17Cr-12Ni, and Fe-20Cr-25Ni stainless steels after mechanical alloying and annealing. *Materials Characterization*, 138, pp.186-194.
124. Shirdel, M., Mirzadeh, H. and Habibi Parsa, M., 2014. Abnormal grain growth in AISI 304L stainless steel. *Materials Characterization*, 97, pp.11-17.
125. Paggi, A., Angella, G. and Donnini, R., 2015. Strain induced grain boundary migration effects on grain growth of an austenitic stainless steel during static and metadynamic recrystallization. *Materials Characterization*, 107, pp.174-181.
126. Di Schino, A., Kenny, J.M. and Abbruzzese, G., 2002. Analysis of the recrystallization and grain growth processes in AISI 316 stainless steel. *Journal of materials Science*, 37(24), pp.5291-5298.
127. Kisko, A., Talonen, J., Porter, D.A. and Karjalainen, L.P., 2015. Effect of Nb microalloying on reversion and grain growth in a high-Mn 204Cu austenitic stainless steel. *ISIJ International*, 55(10), pp.2217-2224.
128. Naghizadeh, M. and Mirzadeh, H., 2016. Elucidating the effect of alloying elements on the behavior of austenitic stainless steels at elevated temperatures. *Metallurgical and Materials Transactions A*, 47(12), pp.5698-5703.
129. Gottstein, G. and Shvindlerman, L.S., 2009. Grain boundary migration in metals: thermodynamics, kinetics, applications. CRC press.
130. Yamamoto, S., Sakiyama, T. and Ouchi, C., 1987. Effect of alloying elements on recrystallization kinetics after hot deformation in austenitic stainless steels. *Transactions of the Iron and Steel Institute of Japan*, 27(6), pp.446-452.
131. Savaedi, Z., Motallebi, R., Mirzadeh, H., Mehdiavaz Aghdam, R. and Mahmudi, R., 2023. Superplasticity of fine-grained magnesium alloys for biomedical applications: A comprehensive review. *Current Opinion in Solid State and Materials Science*, 27(2), p.101058.
132. Shahmir, H., Naghdi, F., Pereira, P.H.R., Huang, Y. and Langdon, T.G., 2018. Factors influencing superplasticity in the Ti-6Al-4V alloy processed by high-pressure torsion. *Materials Science and Engineering: A*, 718, pp.198-206.
133. Bhatta, L., Pesin, A., Zhilyaev, A.P., Tandon, P., Kong, C. and Yu, H., 2020. Recent development of superplasticity in aluminum alloys: A review. *Metals*, 10(1), p.77.
134. Alizadeh, R., Mahmudi, R., Pereira, P.H.R., Huang, Y. and Langdon, T.G., 2017. Microstructural evolution and superplasticity in an Mg-Gd-Y-Zr alloy after processing by different SPD techniques. *Materials Science and Engineering: A*, 682, pp.577-585.
135. Asghari-Rad, P., Nili-Ahmadabadi, M., Shirazi, H., Hossein Nedjad, S. and Koldorf, S., 2017. A significant improvement in the mechanical properties of AISI 304 stainless steel by a combined RCSR and annealing process. *Advanced Engineering Materials*, 19(3), p.1600663.
136. Guler, Z. and Yapici, G.G., 2021. Application of Novel Constrained Groove Pressing Routes on Austenitic Stainless Steel. *Transactions of the Indian Institute of Metals*, 74(11), pp.2599-2608.
137. Singh, R., Singh, D., Sachan, D., Yadav, S.D. and Kumar, A., 2021. Microstructural Evolution and Mechanical Properties of Constrained Groove-Pressed 304 Austenitic Stainless Steel. *Journal of Materials Engineering and Performance*, 30(1), pp.290-301.
138. Taleff, E.M., Nagao, M., Higashi, K. and Sherby, O.D., 1996. High-strain-rate superplasticity in ultrahigh-carbon steel containing 10 wt.% Al (UHCS-10Al). *Scripta Materialia*, 34(12), pp.1919-1923.
139. Xiong, R., Kwon, H., Karthik, G.M., Gu, G.H., Asghari-Rad, P., Son, S., Kim, E.S. and Kim, H.S., 2021. Novel multi-metal stainless steel (316L)/high-modulus steel (Fe-TiB₂) composite with enhanced specific modulus and strength using high-pressure torsion. *Materials Letters*, 303, p.130510.
140. Savaedi, Z., Mirzadeh, H., Mehdiavaz Aghdam, R. and Mahmudi, R., 2022. Thermal stability, grain growth kinetics, mechanical properties, and bio-corrosion resistance of pure Mg, ZK30, and ZEK300 alloys: A comparative study. *Materials Today Communications*, 33, p.104825.
141. Rezaei, A., Mahmudi, R., Cayron, C. and Loge, R., 2021. Microstructural evolution and superplastic behavior of a fine-grained Mg-Gd-Y-Ag alloy processed by simple shear extrusion. *Materials Science and Engineering: A*, 806, p.140803.
142. Sayari, F., Mahmudi, R. and Roumina, R., 2020. Inducing superplasticity in extruded pure Mg by Zr addition. *Materials Science and Engineering: A*, 769, p.138502.
143. Hoseini-Athar, M.M., Mahmudi, R., Babu, R.P. and Hed-

- ström, P., 2019. Microstructural evolution and superplastic behavior of a fine-grained Mg-Gd alloy processed by constrained groove pressing. *Materials Science and Engineering: A*, 754, pp.390-399.
144. Fakhar, N., Sabbaghian, M., Nagy, P., Fekete, K. and Gubicza, J., 2021. Superior low-temperature superplasticity in fine-grained ZK60 Mg alloy sheet produced by a combination of repeated upsetting process and sheet extrusion. *Materials Science and Engineering: A*, 819, p.141444.
145. Mehrabi, A., Mahmudi, R. and Miura, H., 2019. Superplasticity in a multi-directionally forged Mg-Li-Zn alloy. *Materials Science and Engineering: A*, 765, p.138274.
146. Lancaster, R.J., Jeffs, S.P., Haigh, B.J. and Barnard, N.C., 2022. Derivation of material properties using small punch and shear punch test methods. *Materials & Design*, 215, p.110473.
147. Guduru, R.K., Darling, K.A., Kishore, R., Scattergood, R.O., Koch, C.C. and Murty, K.L., 2005. Evaluation of mechanical properties using shear-punch testing. *Materials Science and Engineering: A*, 395(1-2), pp.307-314.
148. Zergani, A., Mirzadeh, H. and Mahmudi, R., 2020. Evolutions of mechanical properties of AISI 304L stainless steel under shear loading. *Materials Science and Engineering: A*, 791, p.139667.
149. Zergani, A., Mirzadeh, H. and Mahmudi, R., 2021. Finite element analysis of plastic deformation in shear punch test. *Materials Letters*, 284, p.128953.
150. Mahmudi, R. and Sadeghi, M., 2013. Correlation between shear punch and tensile strength for low-carbon steel and stainless steel sheets. *Journal of Materials Engineering and Performance*, 22(2), pp.433-438.
151. Eskandari, M., Zarei-Hanzaki, A. and Abedi, H.R., 2013. An investigation into the room temperature mechanical properties of nanocrystalline austenitic stainless steels. *Materials & Design*, 45, pp.674-681.
152. Wang, X., Jiang, L., Zhang, D., Rupert, T.J., Beyerlein, I.J., Mahajan, S., Lavneria, E.J. and Schoenung, J.M., 2020. Revealing the deformation mechanisms for room-temperature compressive superplasticity in nanocrystalline magnesium. *Materialia*, 11, p.100731.
153. Azizi, A. and Abedi, H.R., 2022. Room temperature compressive superplasticity of low density steel. *Scripta Materialia*, 216, p.114757.
154. Dutta, A., Tung, S.Y., Gupta, S.K., Tsai, M.H. and Nene, S.S., 2023. Room-Temperature Superformability in Novel As-Cast High-Entropy Alloy During Compressive Loading. *Advanced Engineering Materials*, p.2201347. DOI: 10.1002/adem.202201347.